

Predominant air-sea states during coastal marine heatwaves

Robert W. Schlegel^{a,*}, Eric C. J. Oliver^{b,c,d}, Sarah Kirkpatrick^e, Andries Kruger^{f,g}, Albertus J. Smit^a

^a*Department of Biodiversity and Conservation Biology, University of the Western Cape, Private Bag X17, Bellville 7535, South Africa*

^b*ARC Centre of Excellence for Climate System Science, Australia*

^c*Institute for Marine and Antarctic Studies, University of Tasmania, Hobart, Australia*

^d*Department of Oceanography, Dalhousie University, Halifax, Nova Scotia, Canada*

^e*UWA Oceans Institute and School of Plant Biology, The University of Western Australia, Crawley, 6009 Western Australia, Australia*

^f*Climate Service, South African Weather Service, Pretoria, South Africa*

^g*Department of Geography, Geoinformatics and Meteorology, Faculty of Natural and Agricultural Sciences, University of Pretoria, South Africa*

Abstract

As the mean temperatures of the world's oceans increase, it is predicted that marine heatwaves (MHWs) will occur more frequently and with increased severity; however, it is hypothesised that more proximate variables may be responsible for these extreme events. An improved understanding of the mechanisms driving MHWs may allow us to better forecast their occurrence at specific localities. To this end we have utilized atmospheric (ERA-Interim) and oceanographic (BRAN) reanalysis data to examine the air-sea state around southern Africa during coastal (<400 m from the low water mark; measured *in situ*) MHWs. Self-organising maps (SOMs) were used to cluster the mean air-sea states during MHWs into 1 of 9 types to determine the predominant patterns. It was found that warm water forced onto the coast via anomalous ocean circulation was the predominant oceanographic pattern during most MHWs. A range of distinct air temperature and wind patterns were found with warm air temperatures over the continent and strong north-westerly winds featuring most prominently during MHWs. It may therefore be possible to forecast the occurrence of MHWs when such air and sea states are projected to occur simultaneously. The lack of any strong air-sea patterns during roughly one third of the MHWs implies that sub-meso-scale activity may have been responsible for them and that finer scale observations may be necessary to deduce their physical drivers. These findings motivate for the implementation of local scale real-time *in situ* monitoring of at risk coastal locations in conjunction with the development of a forecasting and disaster prevention system.

Keywords: extreme events, coastal, atmosphere, ocean, reanalysis data, *in situ* data, climate change

1. Introduction

The anthropogenically forced warming of air, land, and sea have been widely publicized over the last several decades (e.g. Manabe and Wetherald, 1967; Sawyer, 1972; Hansen et al., 1981; Cox et al., 2000; Rosenzweig et al., 2008). Investigations into the negative impacts this warming may have on

*Corresponding author

Email address: 3503570@myuwc.ac.za (Robert W. Schlegel)

5 ecosystems ranges in focus from long term trends (e.g. Scavia et al., 2002; Walther et al., 2002; Burrows
et al., 2011) to shifting states (e.g. Travis, 2003; Grebmeier, 2006; Blamey et al., 2015) to extreme
individual events (e.g. Easterling et al., 2000; Barrett et al., 2008; Wernberg et al., 2012). Whereas long
term temperature trends are projected to have a negative impact on many of earth’s systems (Stocker
et al., 2013), and the shifts in thermal states brought about by these long term trends are projected to
10 cause irreversible species loss (Thomas et al., 2004), extreme events pose a more immediate threat to
ecosystems (e.g. Jolly et al., 2005; Denny et al., 2009; Hufkens et al., 2012). Extreme thermal events
have been given a range of labels but are broadly divided into two categories: cold-spells (e.g. Gunter,
1941; Lirman et al., 2011; Boucek et al., 2016) and heatwaves (e.g. GORDON et al., 1988; Stott et al.,
2004; Perkins-Kirkpatrick et al., 2016). We chose here to focus on heatwaves that occur in the sea,
15 classified as ‘marine heatwaves’ (MHWs).

Several large MHWs, and their ecological impacts, have been well documented. The first of which
being the 2003 Mediterranean MHW that negatively impacted as much as 80% of the Gorgonian fan
colonies (Garrahou et al., 2009). The 2011 Western Australia MHW is now known to have caused a
permanent 100 km range contraction of the ecosystem forming kelp species *Ecklonia radiata* in favour
20 of the tropicalisation of reef fishes and seaweed turfs (Wernberg et al., 2016). The damage caused by
MHWs is not confined to demersal organisms or coastal ecosystems as demonstrated by a MHW in the
North West Atlantic Ocean in 2012 that impacted multiple commercial fisheries (Mills et al., 2013).
When extreme enough, such as “the Blob” that persisted in the North West Pacific Ocean from 2014
to 2016, a MHW may even negatively impact marine mammals and seabirds (Cavole et al., 2016).
25 Analysis of *in situ* coastal seawater temperature time series from South Africa has shown that MHWs
of comparable magnitude to those highlighted here have occurred (Schlegel et al., 2017) however, it
is not known what damage these events may have caused as little long-term ecological sampling is
carried out in the locations of these events.

It is possible to directly compare MHWs occurring anywhere on the globe during any time of year
30 because of a definition developed by Hobday et al. (2016), which was accompanied by the development
of a statistical methodology for their calculation. Whereas the metrics created for the measurement
of MHWs allowed for the comparison of events, they did not directly reveal what may be causing
said events. Beyond common measurements, it is necessary to identify the possible physical drivers of
MHWs so as to be able to compare similar ‘types’ of events and to be able to move towards a system
35 of prediction.

It has been assumed that MHWs should either be caused by oceanic forcing, atmospheric forcing,
or a combination of the two however, the scale at which this forcing must occur in order to drive
MHWs has yet to be determined. Recent research into the development of a mechanistic understanding
between local- *vs.* meso-scale influences on the formation of coastal MHWs has revealed that meso-scale
40 oceanic forcing from offshore onto the nearshore (<400 m from the coast) is far less responsible for
the formation of MHWs than hypothesized (Schlegel et al., 2017). It is therefore necessary to consider
additional mechanisms that may be responsible for these events. For example, the 2011 Western

Australia MHW (Pearce and Feng, 2013) was caused by the aseasonal transport of warm water onto the coast due to a surge of the Leeuwin Current (Feng et al., 2013; Benthuisen et al., 2014). Conversely, Garrabou et al. (2009) were able to show that atmospheric forcing played a clear role in formation of the 2003 Mediterranean MHW. While more complex, Chen et al. (2015) also showed that air-sea heat flux could be attributed as the main forcing variable in the 2012 Atlantic MHW. “The Blob” however appears to have occurred due to the lack of advection of heat from surface waters into the atmosphere due to anomalously high sea level pressure (Bond et al., 2015). Outside of these few examples for well these documented events there has been little progress in developing a global understanding of the forcing of MHWs more broadly.

In order to investigate the potential air and/ or sea influence on coastal MHWs an index of mean synoptic air-sea states during the occurrence of these events was created. These states were then clustered with the use of a self-organising map (SOM). The aim of the clustering of the synoptic air-sea states was to visualise patterns in the air and/ or sea that occur during MHWs at coastal sites. We hypothesized that i) air and sea mesoscale patterns would be revealed through clustering; ii) these patterns would be more distinct in the sea than in the air; and iii) the air-sea states would aid in the development of a broader mechanistic understanding of the physical drivers of coastal MHWs.

2. Methods

2.1. Study region

The *ca.* 3,100 km long South African coastline provides a natural laboratory for investigations into the offshore forcing of nearshore phenomena as it may be divided into three distinct sections, allowing for a range of meso-scale oceanographic influences to be considered within the same research framework (Figure 1). The entire west coast section of the country is distinct from the other two in that it is the realm of the Benguela Current, which forms an Eastern Boundary Upwelling System (EBUS) (Hutchings et al., 2009). Conversely, the east coast section is dominated by the Agulhas Current (Lünning, 1990), a poleward flowing body of warm water. Trapped between these two mighty currents the south coast section is consistently tumultuous. Because this section is also bordered by the Agulhas current it is more closely affiliated to the east coast than the west. The south coast nonetheless experiences both sheer forced and wind driven upwelling in addition to having significantly more thermal variability than either of the other two sections (Schlegel et al., 2017). The range of temperatures experienced along all three sections are large and the gradient of increasing temperature as one moves from the border of Namibia to the border of Mozambique is nearly linear. For a more detailed description of these sections see Smit et al. (2013). The extent of the study area used here was 10°E to 40°E and 25°S to 40°S.

2.2. Data

(RWS: Delete the following...) The temperature dataset used for the calculation of the MHWs consisted of daily temperature records collected *in situ* at dozens of locations. The state of the sea, both SST

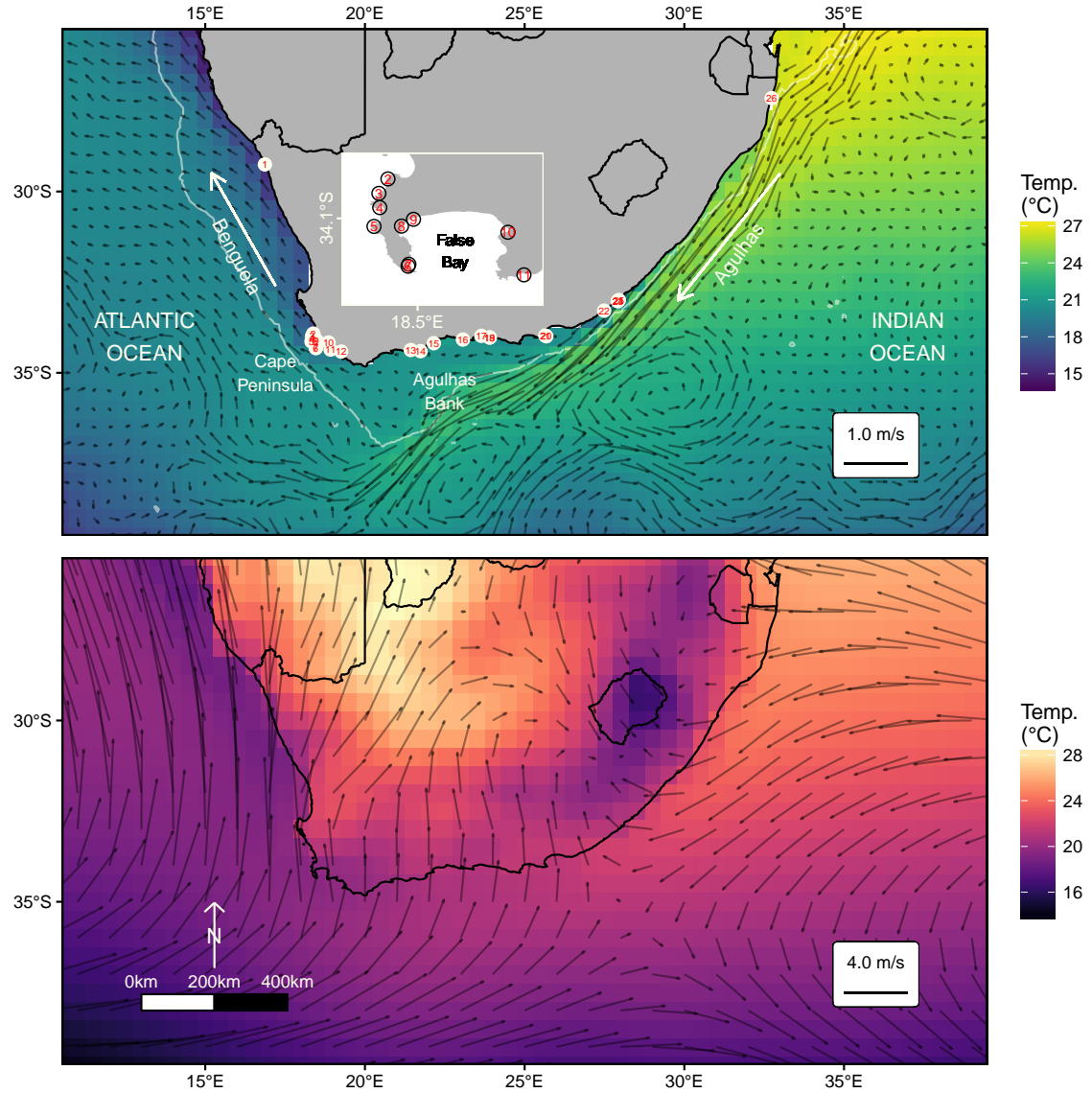


Figure 1: (RWS: This figure is a place holder from the previous paper and I will need to create a new map for this paper. I need to add nation borders as well as any other locations mentioned in the text. I will create a two panel map that shows air and sea with vectors etc. from the ERA and BRAN data.) Map of southern Africa showing bathymetry and the location of the *in situ* temperature time series used in this study shown with circles. The inset maps show detail of the Cape Peninsula/ False Bay area and the Port Alfred region where site labels are obscured due to overplotting of symbols.

and surface currents, were determined with the Bluelink ReANalysis (BRAN; wp.csiro.au/bluelink). The
80 state of the air temperature and winds were determined with ERA-Interim (<http://www.ecmwf.int/en/research/climate-reanalysis/era-interim>).

2.2.1. In situ data

The coastal seawater temperature data used in this study were acquired from the South African Coastal Temperature Network (SACTN, <https://github.com/ajsmit/SACTN>, <https://robert-schlegel.shinyapps.io/SACTN>).
85 The SACTN data are contributed by seven different organizations and are collected *in situ* with a mixture of hand-held alcohol & mercury thermometers as well as digital underwater temperature recorders (UTRs). This data set currently consists of 135 daily time series, with a mean duration of 19.7 years. Therefore many of the time series in this dataset are shorter than the 30 year minimum proscribed for the characterization of marine heatwaves (MHWs, see 'Marine heatwaves' section below)
90 (Hobday et al., 2016), with many having gaps of missing data above the recommended limit of 10%, too (RWS: This 10% claim needs citation. Refer to your previous paper.). It is however deemed necessary to use these data when investigating extreme events in the nearshore (<400 m from the low tide mark) as satellite derived sea surface temperature (SST) values along the coast have been shown to display large biases (Smit et al., 2013) or capture minimum and maximum temperatures poorly (Smale
95 and Wernberg, 2009; Castillo and Lima, 2010). Whereas a 30 year period is ideal for determining an accurate climatology, ten years serves as an acceptable bottom limit (cite). Accounting for these 10 year length and 10% missing data constraints, the total *in situ* time series used in this study was reduced to 26, with a mean length of 22.3 years. Table 3 shows the metadata for the SACTN time series used in this study.

100 2.2.2. Reanalysis data

To visualise a synoptic view of the air-sea state during coastal marine heatwaves (MHWs) (see sections 'Marine heatwaves' and 'Air-sea state' below) it was necessary to use reanalysis products to provide air or sea temperatures with wind/ current vectors in a single product.

The 1/10° Bluelink ReANalysis product was chosen to investigate the state of the sea around
105 southern Africa during coastal MHWs. This modelled product relies on the assimilation of an array of data collected *in situ* and remotely. This representation of the sea state on the scale of 10's of kms is appropriate for the identification of meso-scale events. From this product were taken the sea surface temperature (SST) and surface currents for the study region. BRAN is available for download via XML and is a product of the CSIRO (<https://www.csiro.au/>).

110 The state of the atmosphere was determined with the use of the ERA-Interim reanalysis product, which is produced by the European Centre for Medium-Range Weather Forecasts (ECMWF, <http://www.ecmwf.int/>). These variables used for this study were the surface temperature (2 m) and winds (10 m) and were downloaded at a resolution of 1/2°. (RWS: Change the layer names to those found on the website for better reproducibility.).

115 To ensure even sampling of the synoptic air and sea states the BRAN data were averaged on a

1/2° grid. The data were then trimmed to contain the same longitude and latitude extents. All variables were then reprocessed into the same data frame format for consistent analysis. The BRAN2016 reanalysis product at the writing of this paper was available from January 1st, 1994 to August 31st, 2016. This is less than the range of data currently available for ERA-Interim at January 1st, 1979 to December 31st, 2016. All dates occurring outside of those in the BRAN product were excluded. The analysis period for the climatologies for the BRAN and ERA-Interim data was January 1st, 1979 to December 31st, 2016.

The SST and surface current data from BRAN were used to visualise and quantify the synoptic sea states within the study area. The air temperature and wind data from ERA-Interim were used likewise for the air state.

2.3. Marine heatwaves

The term marine heatwave differs slightly from the definition of a heatwave (HW) originally developed for atmospheric science (Perkins and Alexander, 2013). We use here the definition given by Hobday et al. (2016) as “a prolonged discrete anomalously warm water event that can be described by its duration, intensity, rate of evolution, and spatial extent”.

We use the methodology laid out in Hobday et al. (2016) for the analysis of MHWs in this research. The algorithm developed by Hobday et al. (2016) isolates MHWs by finding the days in which the temperature of a given locality exceeds the 90th percentile of temperatures found there, based on an 11-day moving window. Perkins and Alexander (2013) concluded that the minimum duration for the analysis of atmospheric heatwaves was 3 days. Hobday et al. (2016) found that a minimum length of 5 days allowed for more uniform global results in event detection, leading them to conclude that this would be a better default starting point for MHW detection. Previous work by Schlegel et al. (2017) showed that the inclusion of these much shorter days may lead to spurious connections between events found across different datasets. In this research we are interested in deducing the air-sea state patterns during very large MHWs. We found that eliminating events shorter than 15 days in length caused the removal of 847 of the 976 total MHWs detected in the *in situ* dataset (RWS: Need to give a better reason here.). The events that occurred before or after the reanalysis period were also excluded. This left us with 98 events over a 20 year period. It must also be highlighted that any of the aforementioned 98 MHWs that had ‘breaks’ below the 90th percentile threshold lasting ≤ 2 days followed by subsequent days above the threshold were considered as one continuous event (Hobday et al., 2016).

In order to calculate a MHW it is necessary to supply a climatology against which daily values may be compared. It is proscribed in Hobday et al. (2016) that this period be at least 30 years. Because 20 of the 26 time series used here are below this threshold we have opted to use the first and last complete years of data for each individual time series as the boundaries of the climatological period. Using fewer than 20 years of data to determine a climatology prevents the accurate inclusion of any decadal scale variability (Schlegel and Smit, 2016) however, by using at least 10 years of data we are able to establish a baseline climatology to calculate MHWs (Schlegel et al., 2017). By calculating MHWs against the daily climatologies from their time series in this way the amount they differ from their localities may

Table 1: The descriptions for the metrics of MHWs as proposed by Hobday et al. (2016) and taken from Schlegel et al. (2017).

Name [unit]	Definition
Count [no. events per year]	n : number of MHWs per year
Duration [days]	D : Consecutive period of time that temperature exceeds the threshold
Maximum intensity [$^{\circ}\text{C}$]	i_{max} : highest temperature anomaly value during the MHW
Mean intensity [$^{\circ}\text{C}$]	i_{mean} : mean temperature anomaly during the MHW
Cumulative intensity [$^{\circ}\text{C}\cdot\text{days}$]	i_{cum} : sum of daily intensity anomalies over the duration of the event

be quantified and compared across time and space. Meaning that this allows researchers to examine events from different variability regimes (i.e. regions of the world) and compare them with a consistent set of MHW metrics. The definitions for the metrics that will be focused on in this paper may be found in Table 1.

We calculated the MHWs in the SACTN dataset with the use of the R package ‘RmarineHeatWaves’, which may be downloaded via CRAN (<https://cran.r-project.org/web/packages/RmarineHeatWaves/index.html>), with the developmental version available on GitHub (<https://github.com/ajsmit/RmarineHeatWaves>). The original algorithm used in Hobday et al. (2016) is available for use via python and may be found at <https://github.com/ecjoliver/marineHeatWaves>.

It is necessary to emphasise that MHWs as defined here exist against the daily climatological means of the time series in which they are found and not by exceeding an arbitrarily chosen static threshold. Therefore, one may just as likely find a MHW during winter months as summer months. This is a valuable characteristic of this method of investigation because aseasonal warm winter waters may have deleterious effects on relatively thermophobic species (Wernberg et al., 2011), while concurrently aiding the recruitment or establishment con-specific species (cite).

2.4. Air-sea states

(RWS: This paragraph needs to be rewritten so as to be more clear on how the synoptic states were created.) The synoptic air-sea state during each coastal MHW was created by averaging the SST, air temperature, wind and current (U and V vectors) values from the BRAN and ERA-Interim products at a $1/2^{\circ}$ (pixel) resolution for each day found within the start and end date of each individual event for the entire study area. This allows for possible teleconnections between different coastal sections to be visualised in the study. In order to create anomaly values for the synoptic states a daily climatology of the Julian day for each variable within each pixel was calculated using the same 11-day moving window used to determine seasonal climatologies for MHWs. This provided 366 mean air-sea states that could be subtracted from the daily air-sea values during a coastal MHW in order to create the anomaly values. An example average synoptic air-sea state during one of the largest MHWs in the SACTN dataset is shown in Figure 2.

2.5. Cluster analysis

(RWS: Change subsection header to SOM if the other cluster analysis work is not to be included in the manuscript.) There have been several methods employed in climate science to cluster synoptic

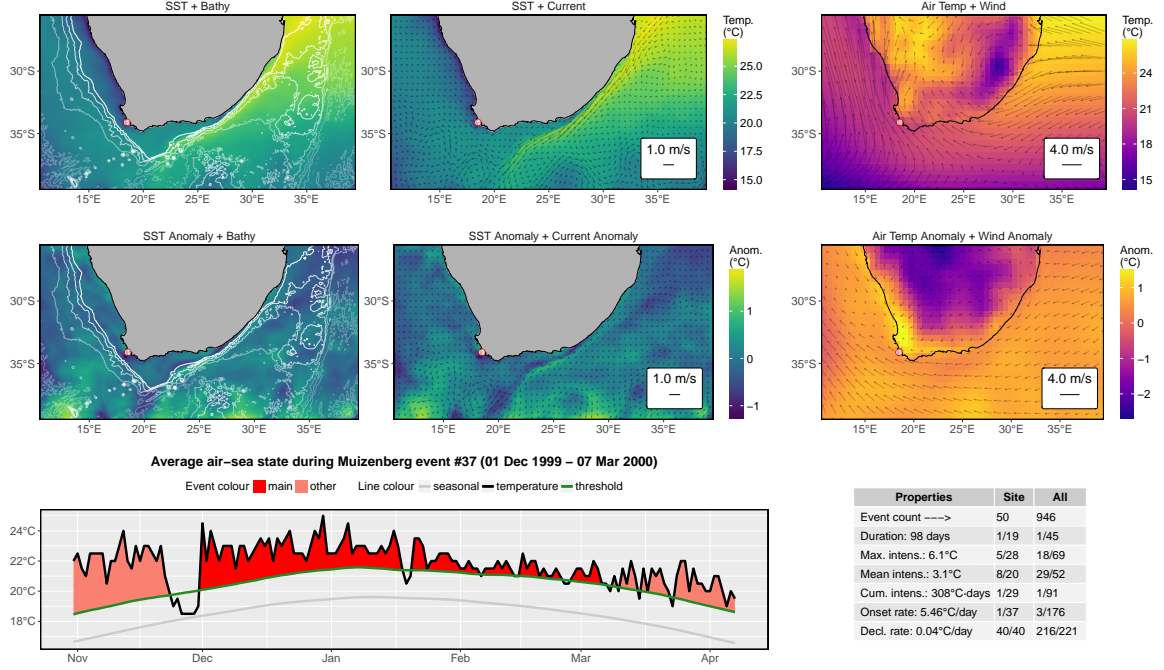


Figure 2: Synoptic air and sea states during a marine heatwave (MHW).

air and or sea states. Most commonly in the past K-means clustering (e.g. Corte-Real et al., 1998; Burrough et al., 2001; Kumar et al., 2011) or, to a lesser extent, hierarchical cluster analysis (HCA) (e.g. Unal et al., 2003) have been used. Though already decades old, the use of self-organising maps (SOMs) has been gaining in popularity in climate studies over only the past several years (e.g. Cavazos, 2000; Hewitson and Crane, 2002; Morioka et al., 2010). As it is outside of the focus of the research presented here, we will not go into detail on the differences in the results generated by the three aforementioned methods. We will state however that it was the SOMs that best clustered out the data when all methods were visualised in two dimensions via a principal component analysis (PCA) (RWS: Consider moving this to results). In addition to the superior pattern recognition displayed by the SOM method, the orientation of the nodes (clusters) as produced by the SOM is also of use to the interpretation of the results of this work.

The initialisation of a SOM is similar to more traditional clustering techniques in that K random points are chosen and from there the data points from the given dataset are re-oriented in an iterative process to reduce the within group sum of squares (Jain, 2010). SOMs differ from more traditional methods in that they also account for the stress of the clustered values in relation to one another and endeavour to orient the nodes (clusters) into the least stressful position possible within a two dimensional space (cite). (RWS: This section may still require fleshing out.)

The daily anomalies during each of the separate 98 events for both air and sea states were averaged to create one mean air-sea state for each event. These synoptic air-sea states were then converted into single vectors with each pixel represented by one column. All 98 vectors representing each MHW were combined into one dataframe to allow for them to be used in a cluster analysis.

205 Because the synoptic air-sea states during each MHW consist of over 9,000 pixels it is difficult for a computer algorithm to arrive satisfactorily at a consistent answer each time the analysis is run (RWS: Better explain this. Also be more explicit with the type of data used, i.e. anomalies). For this reason we opted out of using random initialization (RI) for our SOM models in favour of principal component initialization (PCI). PCI differs from RI in that it uses the two principal components of the dataset, as
 210 determined from a principal component analysis (PCA) to initialize the choice of node centres for the SOM. This allows the SOM model to create the exact same result whenever it is run on the same data. (RWS: It may be necessary to validate the PCA in more detail here.)

The appropriate number of nodes (clusters) to use in a cluster analysis is well known to be a contentious decision. We have chosen here to use 9 nodes for a number of reasons. The first reason was
 215 that SOMs are best run on even grids of data (e.g. 2x3, 3x3, 4x4, etc.) (RWS: cite why even grids are best). Calculating the within group sum of squares (WGSS) value as more nodes were included showed that 4 could be satisfactory, but that at least 6 would be better. By comparing the results of the K-means and HCA also performed on these data (not included here) with the SOM results it became clear that 7 or more nodes (clusters) was appropriate (RWS: Consider deleting all of this and rather
 220 not talk about the other clustering/ ordination tests). Ultimately we settled on 9 nodes as this allowed for a wider variety of different synoptic air-sea states to be separated out from one another, allowing for a better understanding of the dominant air-sea states that exist during coastal MHWs to be formed. A final consideration for the validity of the choice of nodes, as proposed in Johnson (2013), is that the nodes must be significantly different from one another. Using an analysis of similarity ($p=xxx$) we
 225 found this to be true for the choice of 9 nodes. (RWS: Move this last sentence to results after re-writing this paragraph)

Once each event was clustered into 1 of 9 nodes, the synoptic air-sea state for each node was calculated by taking the average for each pixel for each variable from all of the mean air-sea states for each MHW, as outlined in the 'Air-sea states' section above, for that node. Ambroise et al. (2000)
 230 and Ramos (2001) provide examples for the use of multiple clustering techniques for categorizing climate data. We felt it was unnecessary to use more than one technique for the clustering of the events however, we did find that the use of other clustering and ordination methods did help to inform this decision.

2.6. Normal days

235 A necessary consideration (RWS: Motivate for why this is necessary) for the investigation of air-sea states during coastal MHWs is to ensure that they differ from 'normal' air-sea states. In order to compare the normal against the extreme, multi-dimensional scaling (MDS) was performed on the daily climatologies together with the mean air-sea states during the 98 MHWs used here. Furthermore, HCA was applied to all of these combined data with a cutoff at four groups, presumably one for each season.
 240 (RWS: Better explain that 4 clusters was used with the express purpose of forcing the four seasons to materialise) This then would allow us to see if the events that occurred during a certain season

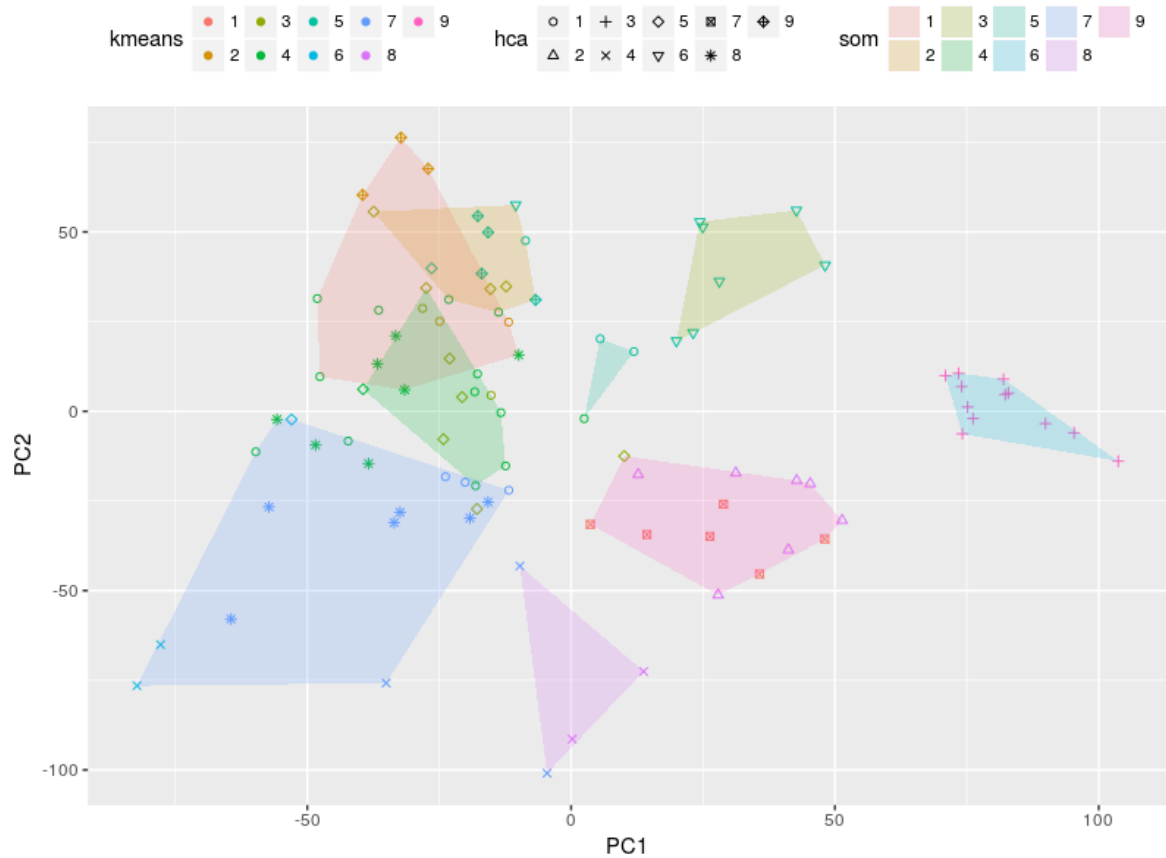


Figure 3: Results for each of three different clustering techniques used to determine the groupings of synoptic air-sea states during coastal MHWs. (RWS: I think I will rather show the results for each technique as separate facets, rather than plotting them together like this.).

would also cluster with the daily air-sea states from those seasons, as well as seeing spatially how these relationships measure out.

3. Results

(RWS: This whole subsection should probably go...)

3.1. Cluster analyses

Due to a lack of consensus in the literature around the best practices for clustering synoptic air-sea states, we decided to compare K-means, HCA and SOM clustering results against one another. Figure 3 shows the results of each clustering technique when each synoptic air-sea state is laid out on a two dimensional plane as determined via a PCA. One may see that the SOM analysis is best able to determine distinct different clusters. Surprisingly HCA appears to produce slightly more distinct clusters than K-means, but both are inferior to the SOM results.

3.2. Air-sea states

(RWS: Merge this with the following section) The 9 most common air-sea states around southern Africa during coastal MHWs may be seen in Figure 4. The top nine panels show the SST and currents, while the bottom 9 panels show the air temperature and winds. All values shown are anomalies. One may note that the patterns in the wind and air temperature states are more clear and pronounced than the SST and currents.

3.3. Nodes

(RWS: Describe each node individually, using the subsections they have been split across as guidelines for what to focus on.) (RWS: Consider finding out which pixels are significantly different from the means within the nodes.)

Immediately apparent in the clustering of the data is that node 6 stands out in starkest contrast to the other nodes the most anomalously warm air and sea states as well as having the strongest winds and currents. As one moves from the right hand nodes to the left they become progressively less intense. With less and less of a pattern present. These left hand nodes serve to show that there are still many coastal MHWs that occur without any strong meso-scale pattern on average. Or at least not a pattern that has occurred often enough over the past 30+ years that would afford them their own node. Due to the vast dissimilarity between the 9 nodes, only 2 events were clustered into the central node. Otherwise the clustering of events into nodes was equitable. Also important to note is that a common pattern in many of the nodes, but particularly node 6, is the abnormal retroflection of the Agulhas current onto the Agulhas Bank (Figure 4).

If we look at the events within the nodes via lolliplots (Figure 5) we see that only one of the nodes shows an air-sea state during primarily one large event that was recorded at multiple locations (node 6). Besides node 6 (and 5), the other nodes consist of a medley of multiple independent events that occurred during different years and seasons, and of varying magnitudes, that cluster together due to their similarity. These nodes represent what a more common air-sea state during a coastal MHW may look like.

3.4. Marine heatwaves

When we look at the mean statistics for each node (Table 2) we see that there is a large difference in the mean duration (days) of MHWs clustered therein. Nodes 4 and 5 show the longest mean durations however, the mean duration in node 5 is skewed by having one very long event and only two total events in that node. Nodes 9 and 2 are characterized by having the shortest MHWs. As large cumulative mean intensities are generally a product of lengthy MHWs, it is not surprising to see that Nodes 4 and 5 also have the highest values for this metric as well. Again though node 5 is misrepresented in this regard due to the one large event clustered there. As for the maximum intensity of events within each node, there is less difference between the nodes than for the other two metrics shown. Nodes 2 and 8 however did have events with the lowest maximum intensities ($^{\circ}\text{C}$) on average.

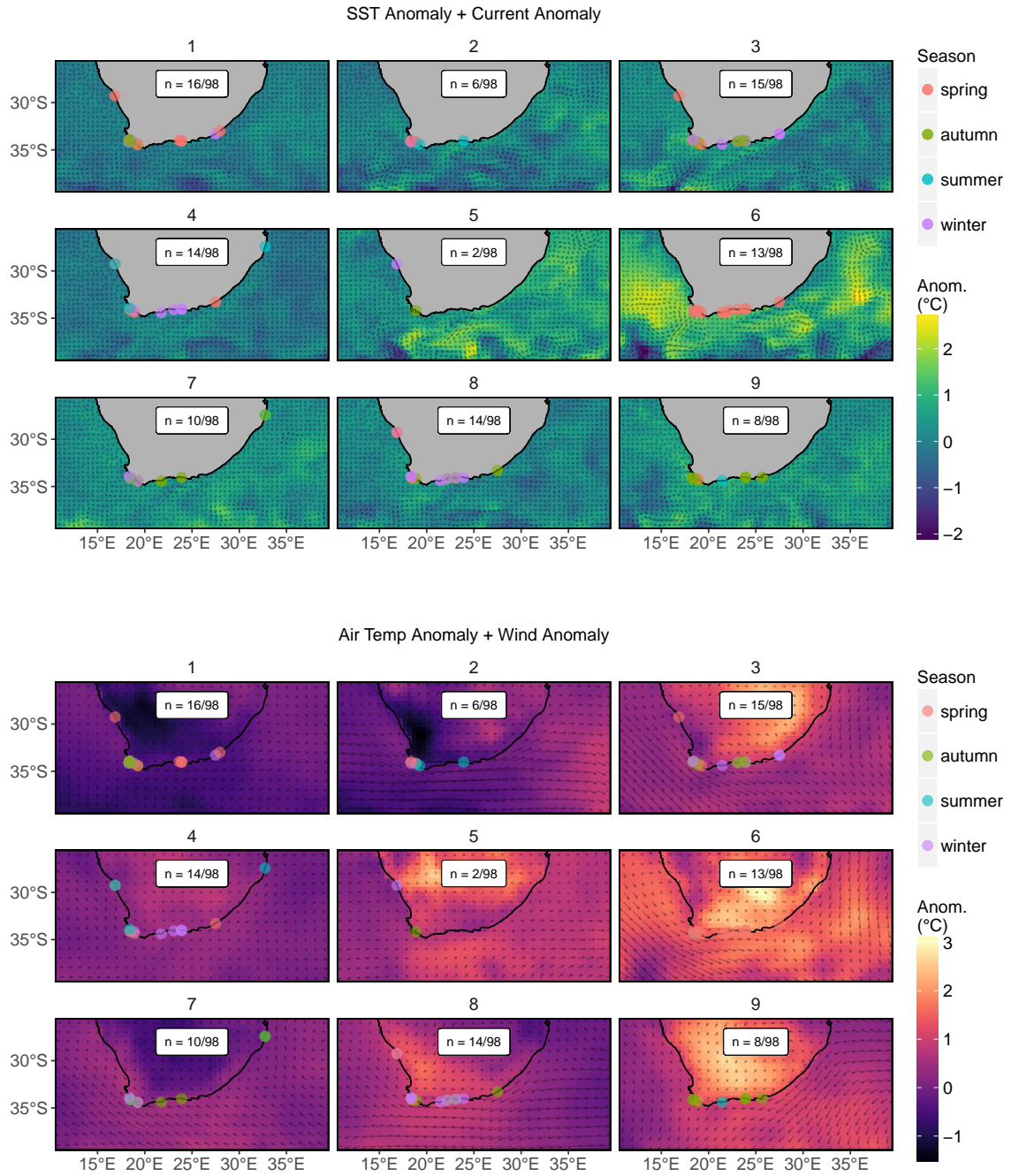


Figure 4: Common air and sea states during coastal marine heatwaves (MHWs). (RWS: I suggest a colourbar that has 0=white, e.g. blue-white-red ditto for air temp below that way we can tell what is cooler than avg and what is warmer than avg. Also improve the vectors for currents.)

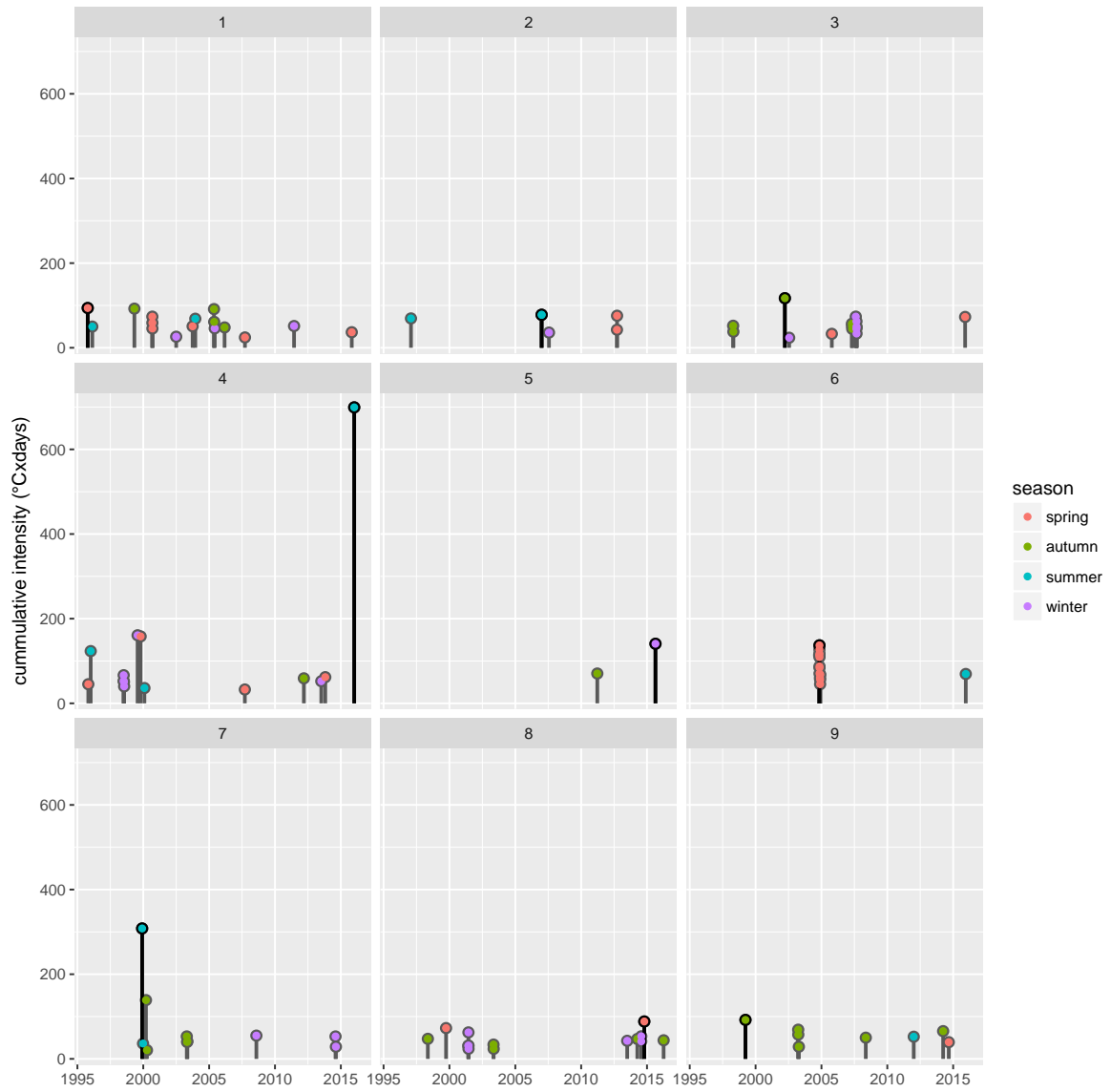


Figure 5: Lollipop plot showing the date during which each event began. The height of each lolli shows the cumulative intensity of the event for comparison of the severity of the events.

Table 2: The relevant metrics and statistics for the events found within each node. (RWS: I will add +- standard deviation to the mean columns)

node	count	summer	autumn	winter	spring	west	south	east	duration_mean	int_cum_mean	int_max_mean
1	16	2	4	3	7	7	8	1	22.20	57.48	3.62
2	6	3	0	1	2	2	4	0	18.50	63.26	4.51
3	15	0	6	7	2	4	11	0	23.70	53.47	3.22
4	14	3	1	6	4	3	10	1	43.50	117.09	3.92
5	2	0	1	1	0	1	1	0	42.00	105.59	4.23
6	13	1	0	0	12	0	13	0	31.20	88.12	4.02
7	10	2	5	3	0	1	7	2	30.00	77.53	3.49
8	14	0	5	7	2	4	10	0	20.20	45.99	3.27
9	8	1	6	0	1	1	7	0	17.50	56.85	4.39
ALL	98	12	28	28	30	23	71	4	27.00	71.14	3.72

3.5. Seasonality

When we consider the seasonal distribution of MHWs in each node, we see that except for node 6, there appears to be no consistency in the season during which a certain air-sea pattern may occur. If we were to plot the air-sea states during MHWs against normal days we see in Figure 6 and Figure 7 that the synoptic air-sea states during the 366 daily climatologies are different from almost all of the synoptic air-sea states during coastal MHWs. As one may see from the flat ellipse of blue squares (the daily climatology points), the variance represented in the x axis is seasonality. Indeed, if the dates are included in the figure above they are in a nearly contiguous state. With January 1st in the top left edge of the ellipse of blue squares with the dates then moving clockwise. May is roughly in the middle of the top of the ellipse and October in the middle on the bottom. The synoptic states during events appear to be controlled by the variance represented by the y axis. This then must be some sort of variance that is aseasonal. Likely the anomalous characteristics of air and or sea that occur during the events. This shows that whatever those states may be, they are independent from the common air-sea states that occur at any time during the year. Also worth noting is that the daily climatologies for summer and winter do not cluster at all with any of the events (Figure 6). They are almost all clustered with autumn, and a few with spring days.

3.6. Spatiality

As shown in Table 2, there are very few events with durations greater than 15 days that occurred in the east coast section of the study area. Therefore it is difficult to judge any potential relationships between synoptic patterns that may be responsible for events only on the east coast, or between the east coast and other sections of the coastline. Table 2 does show that, with the exception of node 6, there are no nodes that contain only events from one coastal section. 8 of the 9 nodes created by the SOM consist of synoptic air-sea states that were occurring during MHWs separated over large distances and by oceanographically dissimilar features.

3.7. Seasonality

4. Discussion

(RWS: Talk more about how the event days cluster out differently from normal days.)

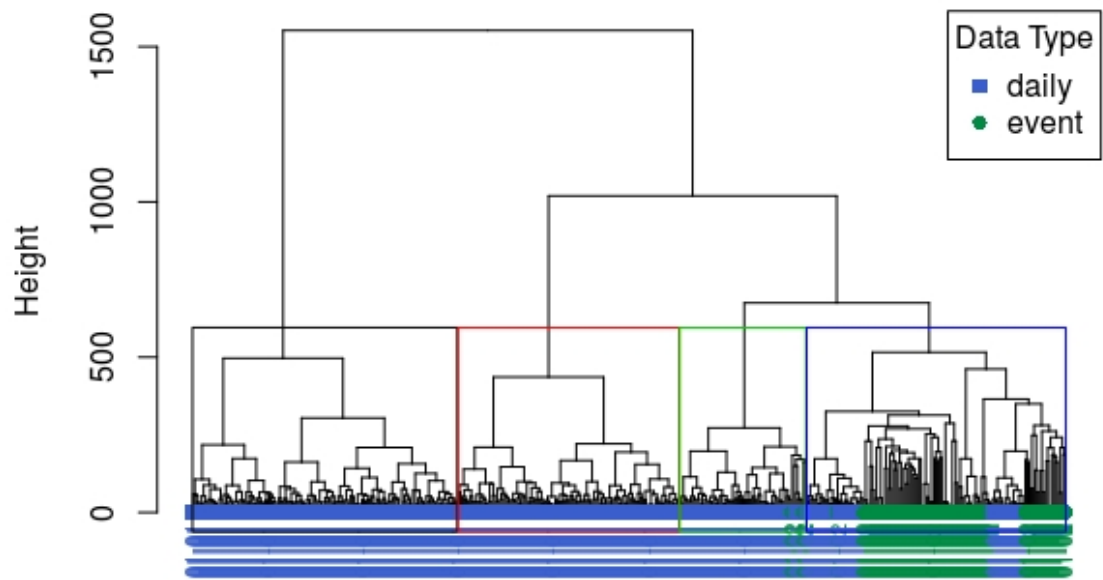


Figure 6: (RWS: I will clean this figure up before submission) Dendrogram showing the distribution of normal daily climatological air-sea states (blue) versus the distribution of mean air-sea states during Marine Heatwaves (MHWs; green). Four clusters are shown as proxies for the four seasons of the year.

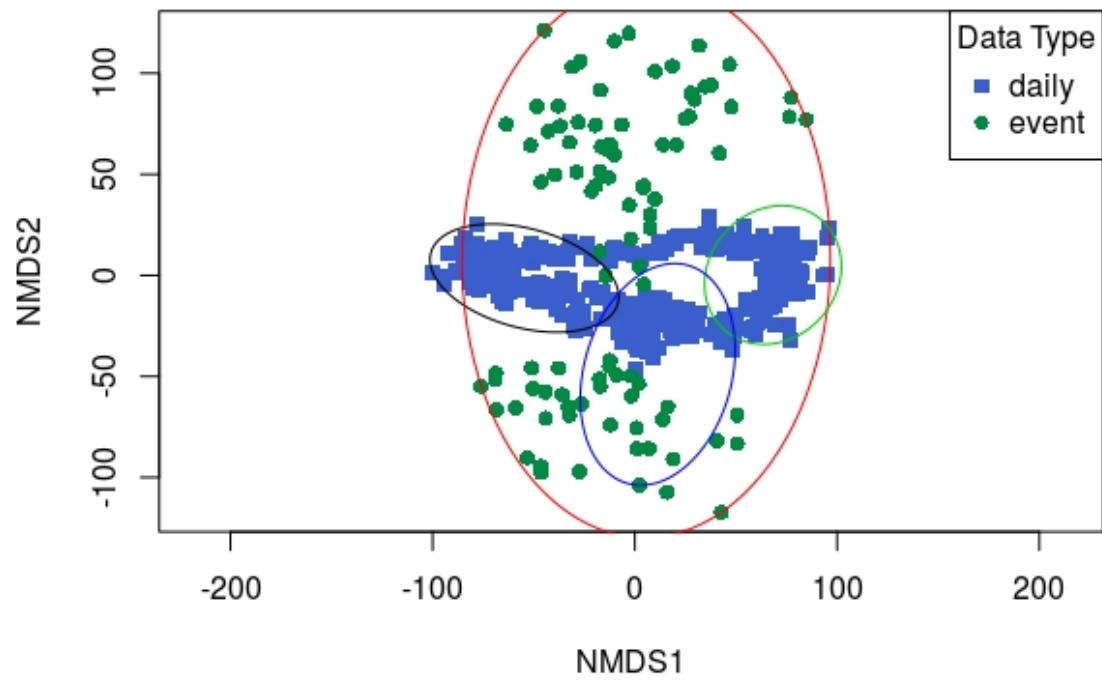


Figure 7: (RWS: I will clean this figure up before submission) Ordiplo showing the distribution of normal daily climatological air-sea states (blue) versus the distribution of mean air-sea states during Marine Heatwaves (MHWs; green). The four clusters from Figure 6 are shown here as ellipsis.

Schaeffer and Roughan (2017) Sub surface MHWs

Beal et al. (2011) Agulhas leakage likely to increase. This is associated with interglacial periods. Whereas the abatement of leakage is associated with severe glacial periods. This is all due to the north or southward shift of westerly winds over the Atlantic.

(RWS: Change this subsection heading.)

4.1. *Anomalous behaviour*

Most notable from the clustering of these events has been the Agulhas current retroflecting (RWS: Talk about Agulhas Leakage instead) north onto the Cape Point region, rather than its usual southward retroflection (cite), when coastal MHWs were detected. This is a similar finding to the cause of the Western Australia MHW (Feng et al., 2013; Benthuyssen et al., 2014). This onshore push of water is most apparent in panel six of Figure 4 however, panels 7, 3 and 9 also show advection of warm water onto the coast around Cape Point (RWS: Consider moving much of this to the results section.). This shows that the anomalously warm temperatures in the areas where MHWs were detected are due to meso-scale activity, and not any local processes. Nodes 8, 4, 1 and 5 lack the apparent onshore forcing of the Agulhas current. These nodes do not show any apparent anomalous behaviour in the sea. When we look at the atmospheric data we see that there are much clearer patterns at play. This supports the argument that some coastal MHWs may be linked more strongly to atmospheric processes than to meso-scale oceanographic forcing.

4.2. *Seasonality*

With the exception of node 6, all of the nodes produced by the SOM contain events not only over large periods of time, but during most if not all four seasons of the year. This means that the meso-scale drivers of MHWs are truly aseasonal. Indeed, as we may see in Figure 7, not only do events occurring during a particular season not relate to the air-sea states during that season, they do not relate to air-sea states during any time of the year. The only small exception to this finding being that some small similarities may be noted during some days in spring and several more during autumn. This implies that whereas air-sea states during events depart from anything seen throughout a normal year, they most closely resemble air-sea states during the tumultuous transitional seasons of spring and Autumn (cite?). (RWS: Calculate the difference in variance between the seasons.)

Also of interest in this study was during which season do MHWs in excess of 15 days tend to occur. We found, to some surprise, that only a small portion (Table 2) of MHWs occurred during summer months. This implies that the phenomena that may be driving these long MHWs occur more often during the cooler months of the year. This may mean that summer months around southern Africa are more stable than at other times of the year, or that the processes that drive long MHWs are linked to the transitioning of warmer temperatures to cooler temperatures. And vice versa. It is not possible to draw any conclusions on this relationship from the output of this research. Further investigation into this possible causal link is required. (RWS: Rather look for cases in the literature in which stable states occur during winter months that could argue for this observation.)

4.3. *Spatiality*

That 8 of the 9 nodes created by the SOM consist of synoptic air-sea states that occurred during MHWs on different coastal sections of the study area leads to two possible implications. (RWS: Rewrite this sentence if you don't simply remove this subsection instead.) The first is that the onshore forcing of the Agulhas current during the MHWs must be extending onto the shore through the Benguela upwelling system. The other implication is that it may be temperature exchange between air and sea at the coast that is leading to these events. (RWS: Must expound upon these two ideas more fully.)

4.4. *Normal days*

Move the above two sections here.

5. Conclusion

This research has highlighted that coastal MHWs with durations in excess of 15 days often occur during the abnormal advection of water onto the coast due to atypical meso-scale activity. In the case of the west and south coast sections of South Africa this offshore water is often warmer than coastal waters and so it was not necessary that the offshore waters be seasonally warm at their point of origin. Anomalous wind and air temperature patterns during coastal MHWs were found to cover a wide range of states and so no one pattern shows a clear relationship to these events.

It was also found that the average synoptic air-sea states found during coastal MHWs do not relate closely to any of the normal air-sea states seen throughout the year. (RWS: Also discuss the atmospheric results.) This means that the meso-scale activity that is occurring during these MHWs is not represented by typical conditions that occur seasonally. Furthermore, the fewest MHWs occurred during summer months than any other season. These two facts taken together support the argument that MHWs are not simply a symptom of solar heating during the warm months of the year, but that other phenomena are having a more pronounced effect on the atypical warming we have documented. (RWS: Now that I think about it, if it is indeed that most MHWs are caused by Agulhas Leakage, the reason there are fewer in the summer would be that coastal temperatures are closer to the Agulhas temperature in the summer. So if there is leakage it wouldn't necessarily show up.)

The mean air-sea state during the longest, most cumulatively intense events (node 4, table 2, fig. 4) was also one of the least anomalous. Meaning that for some of the events which could have potentially had the most negative impact on nearshore ecosystems, there does not appear to be any large scale forcing from the air or sea on coastal waters during those times.

This finding shows that a knowledge of the meso-scale oceanographic and atmospheric properties of an area are necessary to determine what forces may be causing MHWs along a stretch of coastline. But that even with this knowledge, many of the largest MHWs do not show any relationship to these potential meso-scale forces. One must therefore not assume that meso-scale activity in either the air or sea may be at the root of any particularly large MHWs observed in nearshore environments. Finer

spatial resolutions must be considered when investigating such events. This is however challenging as such high resolution *in situ* data are often very sparse.

It is therefore advised that areas of particular susceptibility to MHWs be identified in order to allow for finer scale monitoring of these areas to be supported. Once these areas have been identified and such monitoring systems installed, it may then be possible to better determine what leads to coastal MHWs.

(RWS: Expand on this to better match the abstract.)

Acknowledgements

We would like to thank DAFF, DEA, EKZNW, KZNSB, SAWS and SAEON for contributing all of the raw data used in this study. Without it, this article and the South African Coastal Temperature Network (SACTN) would not be possible. We would also like to thank Dr. Andries Kruger for his contributions to this work. This research was supported by NRF Grant (CPRR14072378735). This paper makes a contribution to the objectives of the Australian Research Council Centre of Excellence for Climate System Science (ARCCSS). The authors report no financial conflicts of interests. The data and analyses used in this paper may be found at <https://github.com/schrob040/MHW>. The Bluelink ocean data products were provided by CSIRO. Bluelink is a collaboration involving the Commonwealth Bureau of Meteorology, the Commonwealth Scientific and Industrial Research Organisation and the Royal Australian Navy.

Supplementary

Meta-data

Further meta-data for each time series and source listed in geographic order along the South African coast from the border of Namibia to the border of Mozambique may be found in Table 3.

References

- Ambroise, C., S??ze, G., Badran, F., Thiria, S., 2000. Hierarchical clustering of self-organizing maps for cloud classification. *Neurocomputing* 30 (1-4), 47–52.
- Barrett, J. E., Virginia, R. A., Wall, D. H., Doran, P. T., Fountain, A. G., Welch, K. A., Lyons, W. B., oct 2008. Persistent effects of a discrete warming event on a polar desert ecosystem. *Global Change Biology* 14 (10), 2249–2261.
- URL <http://doi.wiley.com/10.1111/j.1365-2486.2008.01641.x>
- Beal, L. M., De Ruijter, W. P. M., Biastoch, A., Zahn, R., Cronin, M., Hermes, J., Lutjeharms, J., Quartly, G., Tozuka, T., Baker-Yeboah, S., Bornman, T., Cipollini, P., Dijkstra, H., Hall, I., Park, W., Peeters, F., Penven, P., Ridderinkhof, H., Zinke, J., 2011. On the role of the Agulhas system in ocean circulation and climate. *Nature* 472 (7344), 429–436.
- URL <http://www.nature.com/doifinder/10.1038/nature09983>

Table 3: The metadata and coastal averages for all *in situ* time series used in this study.

	order	site	src	index	lon	lat	depth	type	coast	date.start	date.end	length	N
	84	2	Port Nolloth	SAWS	Port Nolloth/ SAWS	16.87	-29.25	0	thermo	wc	1299.00	16800.00	15502
	100	16	Sea Point	SAWS	Sea Point/ SAWS	18.38	-33.92	0	thermo	wc	1461.00	16527.00	15067
	71	17	Oudekraal	DAFF	Oudekraal/ DAFF	18.35	-33.98	9	UTR	wc	12108.00	16835.00	4728
	41	18	Hout Bay	DEA	Hout Bay/ DEA	18.35	-34.05	28	UTR	wc	7753.00	13992.00	6240
	52	20	Kommetjie	SAWS	Kommetjie/ SAWS	18.33	-34.14	0	thermo	wc	8095.00	16527.00	8433
	12	22	Bordjies	DAFF	Bordjies/ DAFF	18.46	-34.32	4	UTR	sc	12502.00	16748.00	4247
	13	23	Bordjies Deep	DAFF	Bordjies Deep/ DAFF	18.47	-34.31	9	UTR	sc	12087.00	16748.00	4662
	33	27	Fish Hoek	SAWS	Fish Hoek/ SAWS	18.44	-34.14	0	thermo	sc	8095.00	16527.00	8433
	65	29	Muizenberg	SAWS	Muizenberg/ SAWS	18.48	-34.10	0	thermo	sc	1220.00	16527.00	15308
	36	30	Gordons Bay	SAWS	Gordons Bay/ SAWS	18.86	-34.16	0	thermo	sc	986.00	16527.00	15542
	10	31	Betty's Bay	DAFF	Betty's Bay/ DAFF	18.92	-34.36	5	UTR	sc	12765.00	16751.00	3987
	38	32	Hermanus	SAWS	Hermanus/ SAWS	19.25	-34.41	0	thermo	sc	7274.00	16527.00	9254
	109	37	Stilbaai	SAWS	Stilbaai/ SAWS	21.44	-34.37	0	thermo	sc	3652.00	16527.00	12876
	131	38	Ystervarkpunt	DEA	Ystervarkpunt/ DEA	21.74	-34.40	3	UTR	sc	9426.00	13685.00	4260
	61	39	Mossel Bay	DEA	Mossel Bay/ DEA	22.16	-34.18	8	UTR	sc	7846.00	13685.00	5840
	50	42	Knysna	DEA	Knysna/ DEA	23.07	-34.08	7	UTR	sc	9210.00	14554.00	5345
	119	45	Tsitsikamma West	SAWS	Tsitsikamma/ SAWS	23.65	-33.98	0	thermo	sc	7486.00	13559.00	6074
	111	46	Storms River Mouth	SAWS	Storms River Mouth/ SAWS	23.90	-34.02	0	thermo	sc	8491.00	14244.00	5754
	118	47	Tsitsikamma East	DEA	Tsitsikamma/ DEA	23.91	-34.03	10	UTR	sc	7849.00	14558.00	6710
	78	58	Pollock Beach	SAWS	Pollock Beach/ SAWS	25.68	-33.99	0	thermo	sc	10724.00	16527.00	5804
	43	59	Humewood	SAWS	Humewood/ SAWS	25.65	-33.97	0	thermo	sc	1332.00	10956.00	9625
	37	67	Hamburg	DEA	Hamburg/ DEA	27.49	-33.29	4	UTR	sc	9433.00	14667.00	5235
	30	68	Eastern Beach	SAWS	Eastern Beach/ SAWS	27.92	-33.02	0	thermo	ec	5113.00	10438.00	5326
	70	69	Orient Beach	SAWS	Orient Beach/ SAWS	27.92	-33.02	0	thermo	ec	5113.00	16527.00	11415
	68	70	Nahoon Beach	SAWS	Nahoon Beach/ SAWS	27.95	-32.99	0	thermo	ec	5113.00	10438.00	5326
	102	133	Sodwana	DEA	Sodwana/ DEA	32.73	-27.42	18	UTR	ec	8835.00	14636.00	5802

Benthuysen, J., Feng, M., Zhong, L., 2014. Spatial patterns of warming off Western Australia during the 2011 Ningaloo Niño: quantifying impacts of remote and local forcing. *Continental Shelf Research* 91, 232–246.

425 Blamey, L. K., Shannon, L. J., Bolton, J. J., Crawford, R. J., Dufois, F., Evers-King, H., Griffiths, C. L., Hutchings, L., Jarre, A., Rouault, M., Watermeyer, K. E., Winker, H., apr 2015. Ecosystem change in the southern Benguela and the underlying processes. *Journal of Marine Systems* 144, 9–29. URL <http://linkinghub.elsevier.com/retrieve/pii/S092479631400311X>

Bond, N. A., Cronin, M. F., Freeland, H., Mantua, N., may 2015. Causes and impacts of the 2014 430 warm anomaly in the NE Pacific. *Geophysical Research Letters* 42 (9), 3414–3420. URL <http://doi.wiley.com/10.1002/2015GL063306>

Boucek, R. E., Gaiser, E. E., Liu, H., Rehage, J. S., oct 2016. A review of subtropical community resistance and resilience to extreme cold spells. *Ecosphere* 7 (10), e01455. URL <http://doi.wiley.com/10.1002/ecs2.1455>

435 Burrough, P. A., Wilson, J. P., Van Gaans, P. F. M., Hansen, A. J., 2001. Fuzzy k-means classification of topo-climatic data as an aid to forest mapping in the Greater Yellowstone Area, USA. *Landscape Ecology* 16 (6), 523–546.

Burrows, M. T., Schoeman, D. S., Buckley, L. B., Moore, P., Poloczanska, E. S., Brander, K. M., Brown, C., Bruno, J. F., Duarte, C. M., Halpern, B. S., Holding, J., Kappel, C. V., Kiessling, W., 440 O'Connor, M. I., Pandolfi, J. M., Parmesan, C., Schwing, F. B., Sydeman, W. J., Richardson, A. J., nov 2011. The pace of shifting climate in marine and terrestrial ecosystems. *Science* 334 (6056),

652–655.

URL <http://www.sciencemag.org/cgi/doi/10.1126/science.1210288>
<http://www.sciencemag.org/content/334/6056/652.abstract>
445 <http://www.sciencemag.org/content/334/6056/652.full.pdf>

Castillo, K. D., Lima, F. P., 2010. Comparison of in situ and satellite-derived (MODIS-Aqua/Terra) methods for assessing temperatures on coral reefs. *Limnology and Oceanography Methods* 8, 107–117.

Cavazos, T., 2000. Using self-organizing maps to investigate extreme climate events: An application to wintertime precipitation in the Balkans. *Journal of Climate* 13 (10), 1718–1732.

450 Cavole, L., Demko, A., Diner, R., Giddings, A., Koester, I., Pagniello, C., Paulsen, M.-L., Ramirez-Valdez, A., Schwenck, S., Yen, N., Zill, M., Franks, P., 2016. Biological Impacts of the 2013–2015 Warm-Water Anomaly in the Northeast Pacific: Winners, Losers, and the Future. *Oceanography* 29 (2).

URL <https://tos.org/oceanography/article/biological-impacts-of-the-20132015-warm-water-anomaly-i>

455 Chen, K., Gawarkiewicz, G., Kwon, Y.-O., Zhang, W. G., jun 2015. The role of atmospheric forcing versus ocean advection during the extreme warming of the Northeast U.S. continental shelf in 2012. *Journal of Geophysical Research: Oceans* 120 (6), 4324–4339.

URL <http://doi.wiley.com/10.1002/2014JC010547>

Corte-Real, J., Qian, B., Xu, H., 1998. Regional climate change in Portugal: precipitation variability
460 associated with large-scale atmospheric circulation. *International Journal of Climatology* 18 (6), 619–635.

URL [http://onlinelibrary.wiley.com/doi/10.1002/\(SICI\)1097-0088\(199805\)18:6%3C619::AID-JOC271%3E3.0.CO;2-T/abstract](http://onlinelibrary.wiley.com/doi/10.1002/(SICI)1097-0088(199805)18:6%3C619::AID-JOC271%3E3.0.CO;2-T/abstract)
<http://www.scopus.com/scopus/inward/record.url?eid=2-s2.0-3543007704&partnerID=40&rel=R7.0.0>

465 Cox, P. M., Betts, R. a., Jones, C. D., Spall, S. a., Totterdell, I. J., 2000. Acceleration of global warming due to carbon-cycle feedbacks in a coupled climate model. *Nature* 408 (6809), 184–187.

Denny, M. W., Hunt, L. J. H., Miller, L. P., Harley, C. D. G., aug 2009. On the prediction of extreme ecological events. *Ecological Monographs* 79 (3), 397–421.

URL <http://doi.wiley.com/10.1890/08-0579.1>

470 Easterling, D. R., Meehl, G. A., Parmesan, C., Changnon, S. A., Karl, T. R., Mearns, L. O., 2000. Climate extremes: observations, modeling, and impacts. *Science* 289 (5487), 2068–2074.

Feng, M., McPhaden, M. J., Xie, S.-P., Hafner, J., 2013. La Niña forces unprecedented Leeuwin Current warming in 2011. *Scientific Reports* 3, 1277.

Garrabou, J., Coma, R., Bensoussan, N., Bally, M., Chevaldonné, P., Cigliano, M., Diaz, D., Harmelin,
475 J. G., Gambi, M. C., Kersting, D. K., Ledoux, J. B., Lejeusne, C., Linares, C., Marschal, C., Pérez,

T., Ribes, M., Romano, J. C., Serrano, E., Teixido, N., Torrents, O., Zabala, M., Zuberer, F., Cerrano, C., 2009. Mass mortality in Northwestern Mediterranean rocky benthic communities: effects of the 2003 heat wave. *Global Change Biology* 15 (5), 1090–1103.

GORDON, G., BROWN, A. S., PULSFORD, T., dec 1988. A koala (*Phascolarctos cinereus* Goldfuss)
480 population crash during drought and heatwave conditions in south-western Queensland. *Austral Ecology* 13 (4), 451–461.

URL <http://doi.wiley.com/10.1111/j.1442-9993.1988.tb00993.x>

Grebmeier, J. M., mar 2006. A Major Ecosystem Shift in the Northern Bering Sea. *Science* 311 (5766), 1461–1464.

485 URL <http://www.sciencemag.org/cgi/doi/10.1126/science.1121365>

Gunter, G., 1941. Death of fishes due to cold on the Texas coast, January, 1940. *Ecology* 22 (2), 203–208.

Hansen, J., Johnson, D., Lacis, A., Lebedeff, S., Lee, P., Rind, D., Russell, G., 1981. Climate Impact of Increasing Atmospheric Carbon Dioxide. *Science* 213 (4511), 957–966.

490 URL <http://www.sciencemag.org/cgi/doi/10.1126/science.213.4511.957>

Hewitson, B. C., Crane, R. G., 2002. Self-organizing maps: Applications to synoptic climatology. *Climate Research* 22 (1), 13–26.

Hobday, A. J., Alexander, L. V., Perkins, S. E., Smale, D. A., Straub, S. C., Oliver, E. C., Benthuyssen, J. A., Burrows, M. T., Donat, M. G., Feng, M., Holbrook, N. J., Moore, P. J., Scannell, H. A., Sen
495 Gupta, A., Wernberg, T., 2016. A hierarchical approach to defining marine heatwaves. *Progress in Oceanography* 141, 227–238.

Hufkens, K., Friedl, M. A., Keenan, T. F., Sonnentag, O., Bailey, A., O’Keefe, J., Richardson, A. D., jul 2012. Ecological impacts of a widespread frost event following early spring leaf-out. *Global Change Biology* 18 (7), 2365–2377.

500 URL <http://doi.wiley.com/10.1111/j.1365-2486.2012.02712.x>

Hutchings, L., van der Lingen, C. D., Shannon, L. J., Crawford, R. J. M., Verheye, H. M. S., Bartholomae, C. H., van der Plas, a. K., Louw, D., Kreiner, A., Ostrowski, M., Fidel, Q., Barlow, R. G., Lamont, T., Coetzee, J., Shillington, F., Veitch, J., Currie, J. C., Monteiro, P. M. S., 2009. The Benguela Current: an ecosystem of four components. *Progress in Oceanography* 83 (1-4), 15–32.

505 Jain, A. K., 2010. Data clustering: 50 years beyond K-means. *Pattern Recognition Letters* 31 (8), 651–666.

Johnson, N. C., 2013. How many enso flavors can we distinguish? *Journal of Climate* 26 (13), 4816–4827.

Jolly, W. M., Dobbertin, M., Zimmermann, N. E., Reichstein, M., sep 2005. Divergent vegetation growth responses to the 2003 heat wave in the Swiss Alps. *Geophysical Research Letters* 32 (18),

510

n/a–n/a.

URL <http://doi.wiley.com/10.1029/2005GL023252>

Kumar, J., Mills, R. T., Hoffman, F. M., Hargrove, W. W., 2011. Parallel k-means clustering for quantitative ecoregion delineation using large data sets. In: *Procedia Computer Science*. Vol. 4. pp. 1602–1611.

515

Lirman, D., Schopmeyer, S., Manzello, D., Gramer, L. J., Precht, W. F., Muller-Karger, F., Banks, K., Barnes, B., Bartels, E., Bourque, A., Byrne, J., Donahue, S., Duquesnel, J., Fisher, L., Gilliam, D., Hendee, J., Johnson, M., Maxwell, K., McDevitt, E., Monty, J., Rueda, D., Ruzicka, R., Thanner, S., 2011. Severe 2010 cold-water event caused unprecedented mortality to corals of the Florida reef tract and reversed previous survivorship patterns. *PLOS ONE* 6 (8).

520

Lünning, K., 1990. *Seaweds: their environment, biogeography and ecophysiology*. John Wiley and Sons. Wiley, New York (USA).

Manabe, S., Wetherald, R. T., 1967. Thermal Equilibrium of the Atmosphere with a Given Distribution of Relative Humidity. *Journal of the Atmospheric Sciences* 24 (3), 241–259.

URL <http://journals.ametsoc.org/doi/abs/10.1175/1520-0469%7B281967%7D29024%7D3C0241%7D3ATEOTAW%7D0.C0%7D3B2>

525

Mills, K., Pershing, A., Brown, C., Chen, Y., Chiang, F.-S., Holland, D., Lehuta, S., Nye, J., Sun, J., Thomas, A., Wahle, R., 2013. Fisheries Management in a Changing Climate: Lessons From the 2012 Ocean Heat Wave in the Northwest Atlantic. *Oceanography* 26 (2).

URL <https://tos.org/oceanography/article/fisheries-management-in-a-changing-climate-lessonsfrom->

530

Morioka, Y., Tozuka, T., Yamagata, T., 2010. Climate variability in the southern Indian Ocean as revealed by self-organizing maps. *Climate Dynamics* 35 (6), 1075–1088.

Pearce, A. F., Feng, M., 2013. The rise and fall of the "marine heat wave" off Western Australia during the summer of 2010/2011. *Journal of Marine Systems* 111–112, 139–156.

535

Perkins, S. E., Alexander, L. V., 2013. On the measurement of heat waves. *Journal of Climate* 26 (13), 4500–4517.

Perkins-Kirkpatrick, S. E., White, C. J., Alexander, L. V., Argüeso, D., Boschhat, G., Cowan, T., Evans, J. P., Ekström, M., Oliver, E. C., Phatak, A., Purich, A., 2016. Natural hazards in Australia: heatwaves. *Climatic Change* 139 (1), 101–114.

540

Ramos, M. C., 2001. Divisive and hierarchical clustering techniques to analyse variability of rainfall distribution patterns in a Mediterranean region. *Atmospheric Research* 57 (2), 123–138.

Rosenzweig, C., Karoly, D., Vicarelli, M., Neofotis, P., Wu, Q., Casassa, G., Menzel, A., Root, T. L., Estrella, N., Seguin, B., Tryjanowski, P., Liu, C., Rawlins, S., Imeson, A., 2008. Attributing physical

and biological impacts to anthropogenic climate change. *Nature* 453 (7193), 353–357.

URL <http://www.nature.com/doifinder/10.1038/nature06937>

545 Sawyer, J. S., 1972. Man-made Carbon Dioxide and the “Greenhouse” Effect. *Nature* 239 (5366), 23–26.

URL <http://www.nature.com/doifinder/10.1038/239023a0>

Scavia, D., Field, J. C., Boesch, D. F., Buddemeier, R. W., Burkett, V., Cayan, D. R., Fogarty, M., Harwell, M. A., Howarth, R. W., Mason, C., Reed, D. J., Royer, T. C., Sallenger, A. H., Titus, J. G., apr 2002. Climate change impacts on U.S. Coastal and Marine Ecosystems. *Estuaries* 25 (2), 149–164.

550

URL <http://link.springer.com/10.1007/BF02691304>

Schaeffer, A., Roughan, M., 2017. Sub-surface intensification of marine heatwaves off southeastern Australia: the role of stratification and local winds. *Geophysical Research Letters*.

URL <http://doi.wiley.com/10.1002/2017GL073714>

555 Schlegel, R. W., Oliver, E. C. J., Wernberg, T., Smit, A. J., 2017. Nearshore and offshore co-occurrence of marine heatwaves and cold-spells. *Progress in Oceanography* 151, 189–205.

URL <http://dx.doi.org/10.1016/j.pocean.2017.01.004>

Schlegel, R. W., Smit, A. J., 2016. Climate Change in Coastal Waters: Time Series Properties Affecting Trend Estimation. *Journal of Climate* 29 (24), 9113–9124.

560

URL <http://journals.ametsoc.org/doi/10.1175/JCLI-D-16-0014.1>

Smale, D. A., Wernberg, T., 2009. Satellite-derived SST data as a proxy for water temperature in nearshore benthic ecology Peer reviewed article. *Marine Biology* 387, 27–37.

Smit, A. J., Roberts, M., Anderson, R. J., Dufois, F., Dudley, S. F. J., Bornman, T. G., Olbers, J., Bolton, J. J., 2013. A coastal seawater temperature dataset for biogeographical studies: large biases between in situ and remotely-sensed data sets around the coast of South Africa. *PLOS ONE* 8 (12).

565

Stocker, T., Qin, D., Plattner, G. K., Tignor, M., Allen, S. K., Boschung, J., Nauels, A., Xia, Y., Bex, V., Midgley, P. M. (Eds.), 2013. Climate change 2013: the physical science basis: Working Group I contribution to the Fifth Assessment Report of the Intergovernmental Panel on Climate Change. Cambridge University Press, Cambridge, United Kingdom and New York, NY, USA.

570 Stott, P. A., Stone, D. A., Allen, M. R., dec 2004. Human contribution to the European heatwave of 2003. *Nature* 432 (7017), 610–614.

URL <http://www.nature.com/doifinder/10.1038/nature03089>

Thomas, C. D., Cameron, A., Green, R. E., Bakkenes, M., Beaumont, L. J., Collingham, Y. C., Erasmus, B. F. N., de Siqueira, M. F., Grainger, A., Hannah, L., Hughes, L., Huntley, B., van Jaarsveld, A. S., Midgley, G. F., Miles, L., Ortega-Huerta, M. A., Townsend Peterson, A., Phillips, O. L., Williams, S. E., 2004. Extinction risk from climate change. *Nature* 427 (6970), 145–148.

575

URL <http://www.nature.com/doifinder/10.1038/nature02121>

Travis, J. M. J., 2003. Climate change and habitat destruction: a deadly anthropogenic cocktail. *Proceedings of the Royal Society B: Biological Sciences* 270 (1514), 467–473.

580 URL <http://rspb.royalsocietypublishing.org/cgi/doi/10.1098/rspb.2002.2246>

Unal, Y., Kindap, T., Karaca, M., 2003. Redefining the climate zones of Turkey using cluster analysis. *International Journal of Climatology* 23 (9), 1045–1055.

Walther, G.-R., Post, E., Convey, P., Menzel, A., Parmesan, C., Beebee, T. J. C., Fromentin, J.-M., Hoegh-Guldberg, O., Bairlein, F., mar 2002. Ecological responses to recent climate change. *Nature* 416 (6879), 389–395.

585 URL <http://www.nature.com/doi/10.1038/416389a>

Wernberg, T., Bennett, S., Babcock, R. C., Bettignies, T. D., Cure, K., Depczynski, M., Dufois, F., Fromont, J., Fulton, C. J., Hovey, R. K., Harvey, E. S., Holmes, T. H., Kendrick, G. A., Radford, B., Santana-garcon, J., Saunders, B. J., Smale, D. A., Thomsen, M. S., 2016. Climate driven regime shift of a temperate marine ecosystem. *Science* 351 (6282), 1229–1232.

590

Wernberg, T., Russell, B. D., Moore, P. J., Ling, S. D., Smale, D. A., Campbell, A., Coleman, M. A., Steinberg, P. D., Kendrick, G. A., Connell, S. D., 2011. Impacts of climate change in a global hotspot for temperate marine biodiversity and ocean warming. *Journal of Experimental Marine Biology and Ecology* 400 (1-2), 7–16.

Wernberg, T., Smale, D. a., Tuya, F., Thomsen, M. S., Langlois, T. J., de Bettignies, T., Bennett, S., Rousseaux, C. S., 2012. An extreme climatic event alters marine ecosystem structure in a global biodiversity hotspot. *Nature Climate Change* 3 (8), 78–82.

595

URL <http://www.nature.com/doi/10.1038/nclimate1627>